iScience

CellPress
OPEN ACCESS

Article

Niche differentiation of ammonia-oxidizing archaea and related autotrophic carbon fixation potential in the water column of the South China Sea

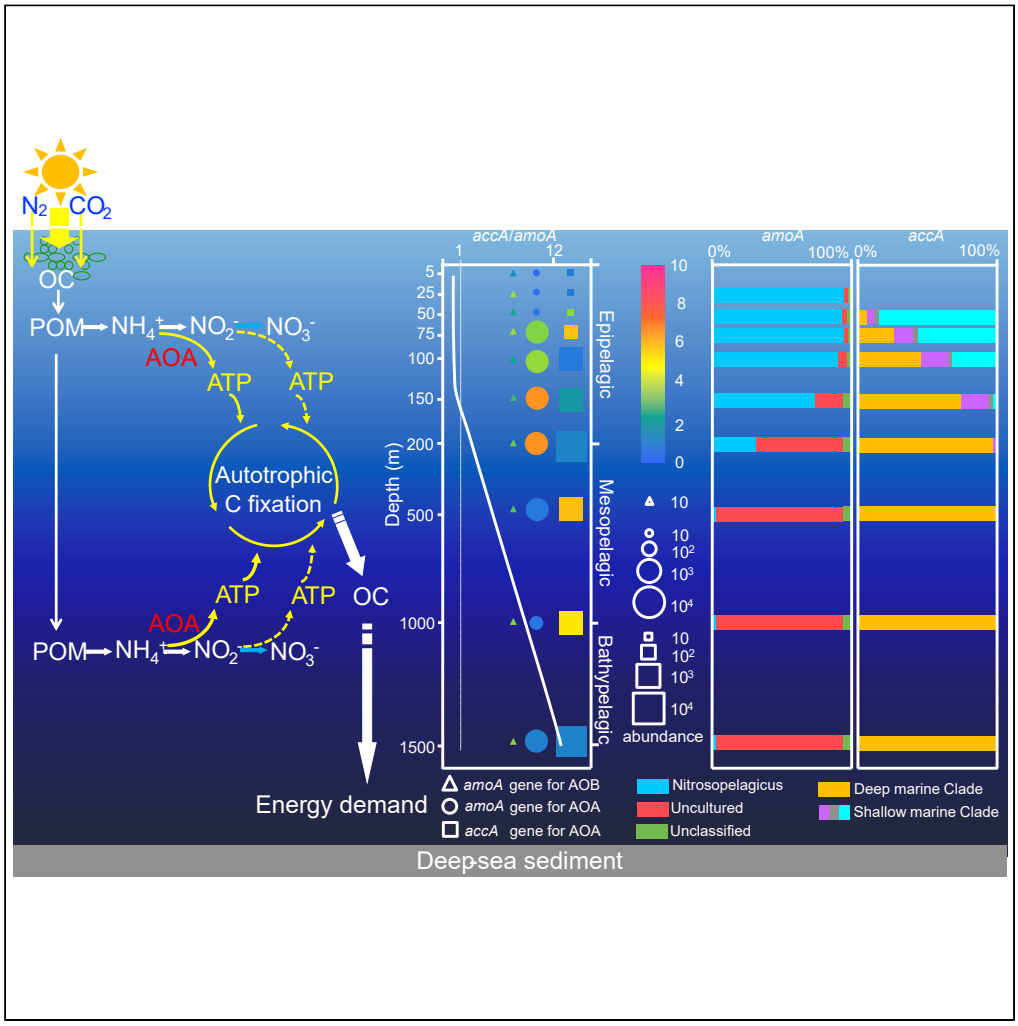

Jiapeng Wu, Yiguo Hong, Xiang He, ..., Fei Ye, Yunhua Yang, Juan Du

yghong@gzhu.edu.cn

Highlights

Higher abundances of AOA were found below the euphotic zone

Higher ratios of *accA*/*amoA* gene were also observed in deep water

Nitrosopelagicus shifted to uncultured genus from surface to deep water

The autotrophic AOA contribute significantly to the primary productivity

Wu et al., iScience 25, 104333
May 20, 2022
https://doi.org/10.1016/j.isci.2022.104333

iScience

CellPress
OPEN ACCESS

Article

Niche differentiation of ammonia-oxidizing archaea and related autotrophic carbon fixation potential in the water column of the South China Sea

Jiapeng Wu,[1,3] Yiguo Hong,[1,2,3,4,*] Xiang He,[1] Xiaohan Liu,[1] Jiaqi Ye,[1] Lijing Jiao,[1] Yiben Li,[1] Yu Wang,[1] Fei Ye,[1] Yunhua Yang,[1] and Juan Du[1]

SUMMARY

The significant primary production by ammonia-oxidizing archaea (AOA) in the ocean was reported, but the carbon fixation process of AOA and its community composition along the water depth remain unclear. Here, we investigated the abundance, community composition, and potential carbon fixation of AOA in water columns of the South China Sea. Higher abundances of the *amoA* and *accA* genes of AOA were found below the euphotic zone. Similarly, higher carbon fixation potential of AOA, evaluated by the ratios of *amoA* to *accA* gene, was also observed below euphotic zone and the ratios increased with increasing water depth. The vertical niche differentiation of AOA was further evidenced, with the dominant genus shifting from *Nitrosopelagicus* in the epipelagic zone to uncultured genus in the meso- and bathypelagic zones. Our findings highlight the higher carbon fixation potential of AOA in deep water and the significance of AOA to the ocean carbon budget.

INTRODUCTION

Oceans store the largest amount of carbon in the biosphere. The ocean productivity accounts for more than half of global productivity, which primarily occurs in the euphotic zone and relies on the autotrophic photosynthetic process by the phytoplankton to fix carbon dioxide (CO_2) (del Giorgio and Duarte, 2002). In contrast, owing to the limitation of light, it is difficult to generate primary productivity in the deep and dark ocean. Particles of organic matter (POM) that sink from the euphotic zone are the main way to meet the demand for the carbon in this energy-starved dark ocean, and the POM are mineralized by microorganisms to produce energy (del Giorgio and Duarte, 2002). Nevertheless, increasing numbers of studies have found that the prokaryotic carbon demand (PCD) was significantly higher than the carbon produced by POM that sinks from the euphotic zone (Carlson et al., 1994; Reinthaler et al., 2006). Furthermore, the imbalance between the energy produced by sinking POM and PCD is becoming problematic as the depth of seawater increases.

Newly produced POM was first detected at a depth of 700–900 m in the north of the Pacific Ocean, which suggests that a new unknown productivity process mediated by bacterial chemolithotrophy could possibly exist in the deep sea (Karl et al., 1984). After that, increased studies found newly produced POM in deep water (Baltar et al., 2009; Reinthaler et al., 2010). The concentration and flux of ammonia (NH_4^+) adsorbed by the sinking POM increased between a depth of 100 and 150 m. In contrast, the contents of NH_4^+ that were found below 150 m gradually decreased as the depth increased, and NO_2^- was formed. The results of an on-board culture experiment showed that there are active autotrophic processes in the depth of 550–750 m where a decrease in NH_4^+ and an increase in NO_2^- were observed. In addition, abundant ammonia-oxidizing bacteria (AOB), primarily species of *Nitrosomonas*, were detected in all the sediments collected from traps using an immunofluorescence technique. A higher cell density of AOB was found after *in situ* culture in a sediment trap, thus confirming the activity of AOB (Karl et al., 1984). These results led Karl et al. (1984) to summarize that the energy transported from the euphotic zone is significantly higher than that stored in the sinking POM, and the ammonia oxidation process may be an important source of energy in the deep sea ecosystem. The carbon produced by the autotrophic processes in deep sea layer contributed 12%–72% of the PCD of the microbial community in the northeast Atlantic (Baltar et al., 2009). Reinthaler et al. (2010) found high rates of carbon fixation (0.1–56.7 mmol m^3 d^{-1}) in the eastern and western

[1]Institute of Environmental Research at Greater Bay Area; Key Laboratory for Water Quality and Conservation of the Pearl River Delta, Ministry of Education, Guangzhou University, Guangzhou 510006, China

[2]School of Environmental Science and Engineering, Guangzhou University, Guangzhou 510006, China

[3]These authors contributed equally

[4]Lead contact

*Correspondence: yghong@gzhu.edu.cn

https://doi.org/10.1016/j.isci.2022.104333

north Atlantic Ocean, and this newly produced carbon is equivalent to 15%–53% of the carbon that sinks from the euphotic zone. Ingalls et al. (2006) used ^{14}C to label the glycerol dialkyl glycerol tetraethers of planktonic archaea to investigate the rate of autotrophic carbon fixation by archaea in the subtropical North Pacific circulation and found that the autotrophic carbon fixation by planktonic archaea below the euphotic zone accounts for 83% of the carbon absorption of all archaea. It is estimated that the productivity of marine planktonic archaea can reach 0.6-0.7 Gt C yr^{-1}, accounting for approximately 1% of the marine primary productivity (50 Gt C yr^{-1}). With the discovery of ammonia-oxidizing archaea (AOA) as the most abundant autotrophic microorganisms currently known in the marine ecosystem, increasing numbers of studies have proven that AOA are important contributors to the primary productivity within the deep sea and play a significant role in the process of autotrophic carbon fixation in the deep sea (Hansman et al., 2009; Herndl et al., 2005; Tetu et al., 2013; Yakimov et al., 2011). However, our knowledge about the role of AOA in carbon fixation in the deep sea remains to be clearly elucidated.

An analysis of a pure culture and the genomic characteristic of *Nitrosomonas europaea* showed that AOB use the Calvin–Benson–Bassham (CBB) cycle during their process of fixing carbon (Chain et al., 2003). RuBisCo is the key enzyme of the CBB cycle, which uses three molecules of ATP and two molecules of NADPH to fix one molecule of CO_2^-. The carbon fixation process of AOB is projected to account for 80% of the energy consumption of the whole cell (Kelly, 1978). In contrast, AOA obtain electrons from NH_4^+ through process of ammonia oxidation, and the electrons are transferred through the electron transport chain to convert the chemical energy stored in NH_4^+ into ATP. AOA produce carbon by consuming ATP and fixing CO_2^- through the 3-hydroxypropionate/4-hydroxybutyrate (3-HP/4-HB) cycle, which is more energy efficient than other autotrophic processes (Blainey et al., 2011; Hallam et al., 2006; Spang et al., 2012; Tourna et al., 2011; Walker et al., 2010). Könneke et al. (2014) found that the AOA *Nitrosopumilus maritimus* increases more biomass than the AOB *Nitrosococcus oceani* while oxidizing the same amount of ammonium. The AOA were hypothesized to have a greater competitive advantage under oligotrophic conditions. Nevertheless, the respective contribution of AOA and AOB to the carbon fixation in the deep sea remains unknown.

Ammonia mono-oxygenase alpha subunit (*amoA*) gene and acetyl-CoA carboxylase α-submit (*accA*) gene are the key functional genes involved in energy and chemoautotrophic CO_2 fixation in AOA, respectively (Tolar et al., 2016; Yakimov et al., 2009, 2011). The diversity and community composition of AOA and AOB were targeted by *amoA* gene (Francis et al., 2005; Rotthauwe et al., 1997). AccA gene has been used successfully for studying the archaeal CO_2 fixation in different ecosystems (Bergauer et al., 2013; Hu et al., 2011a, 2011b; Song et al., 2013; Yakimov et al., 2009, 2011). As regard to the function and distribution pattern of these two genes in the seawater columns, the ratios of *accA* and *amoA* gene abundances have been developed as an important proxy to estimate the carbon fixation potential of AOA (Hu et al., 2011a, 2011b). More recently, Bergauer et al. (2013) found that the abundance of AOA was significantly higher than that of AOB, and AOA is the dominant group of microbes that oxidize ammonia. Rates of ammonia oxidation have been reported in most oceans, including the polar region, and they range from 0–100 nmol day^{-1} (Tolar et al., 2013; Ward, 2008; Yool et al., 2007). Zhang et al. (2020) found that ammonia oxidation processes provided more free energy than nitrite oxidation processes. The carbon fixation rate of nitrifiers was estimated at 2×10^{13} mol C $year^{-1}$ throughout the dark ocean. Furthermore, comparative physiological, metagenomic, and genomic analyses were combined to show the global distribution pattern of AOA and their adaptive radiation into different habitats. Phosphate contents and hydrostatic pressures were recognized as key environmental variables that drive the environmental adaptations of AOA in the ocean (Qin et al., 2020). However, the potential autotrophic carbon fixation and community compositions of *amoA* and *accA* genes of AOA remain unclear.

To more comprehensively understand the potential of AOA to autotrophically fix carbon in the deep sea, we sampled 30 seawater samples in four water columns of the South China Sea (SCS) to (1) distinguish the respective contribution of AOA and AOB to the carbon fixation in deep sea, (2) analyze the carbon fixation potential by comparing the abundances of *amoA* and *accA* genes at different depths, and (3) investigate the community compositions of *amoA* and *accA* genes of AOA.

RESULTS

Physicochemical parameters in water columns of the SCS

The depth profiles of physicochemical parameters, including salinity, temperature, dissolved oxygen (DO), and dissolved inorganic nitrogen (DIN) concentrations, along the water columns in S3, S7, S12, and S18 in

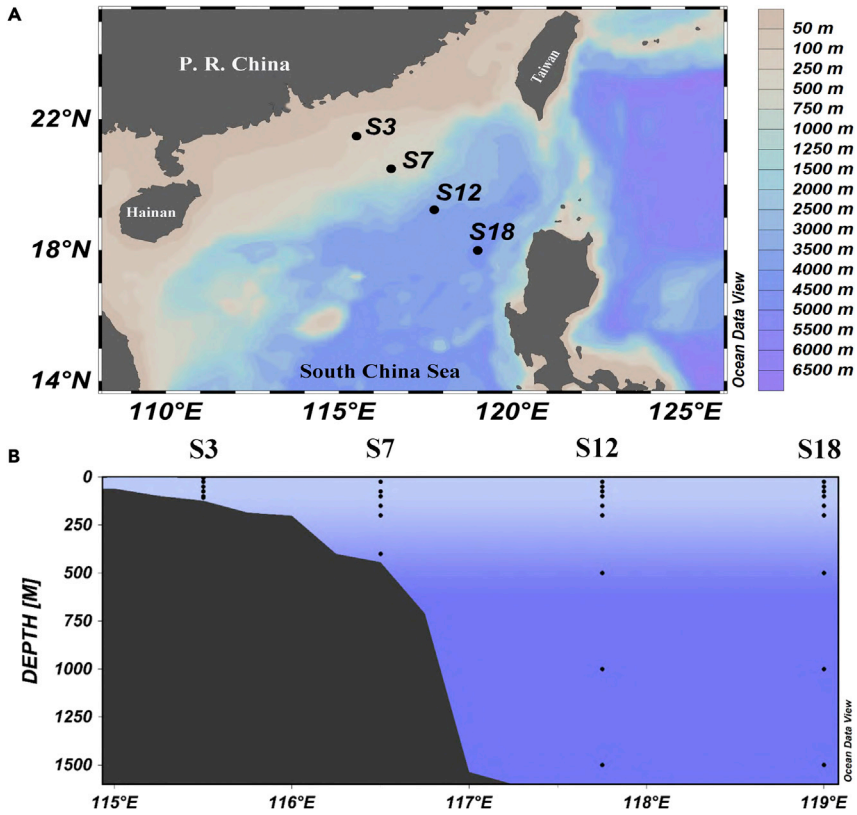

Figure 1. Study sites and sampling stations during the 2016 cruise in the South China Sea (SCS)

(A) Map of sampling stations in the South China Sea.

(B) The sampling depths of all stations.

the SCS (Figure 1) are shown in Figure 2 and Table S1. The sampling depths of the water columns ranged from 5 to 1,500 m. High salinity was observed in all the water samples with values ranging from 30.7 to 34.8‰, and the highest values were found at depths of 150–200 m (Figures 2A–2D, black lines). The temperature profile revealed a sharp decrease from 30°C at the surface water to 2.7°C at a depth of 1,500 m (Figures 2A–2D, red dotted lines). The DO values in the water columns were high and ranged from 80 to 210.11 μmol/L. The DO was found to decrease along the water depth, and the highest values were observed at 50 to 100 m (Figures 2A–2D, blue dotted lines). Increased trends of NO_3^- were observed along the water depth, and the highest values were observed below 150 m (50 m for S3), which ranged from 0.02 to 41.08 μmol/L (Figures 2E–2H, blue dotted lines). NO_2^- contents (ranged from 0.01 to 1.77 μmol/L) were low throughout the depth profiles (Figures 2E–2H, black dotted lines). High concentrations of NH_4^+ were found lower than 150 m (50 m for S3) in the epipelagic water (Figures 2E–2H, red dotted lines). Compared with the contents of NH_4^+ (0.31 ± 0.38 μmol/L, n = 29) and NO_2^- (0.41 ± 0.38 μmol/L, n = 29), NO_3^- (11.08 ± 14.05 μmol/L, n = 29) was the dominant form of DIN (Figures 2E–2H).

Depth profiles and the abundances and diversity of *amoA* gene

A qPCR analysis of *amoA* successfully detected and quantified the abundances of AOA and AOB in all the water samples selected (Figure 3, light blue and dark blue bars). The abundance of AOA ranged from 1.18 ± 0.21 to (3.07 ± 0.58)×10^4 copies mL^{-1}, whereas the abundance of AOB ranged from (1.79 ± 0.17) ×10^1 to (3.99 ± 1.10)×10^2 copies mL^{-1}. The distribution patterns of the abundances of ammonia oxidizing prokaryote (AOP) in these four sampling seawater columns were consistent. Lower abundances of AOA and AOB were detected in the surface water that ranged from 0 to 50 m. The ratios of AOA/AOB in these layers were <1, suggesting that AOB dominates the community of AOP in the epipelagic zone. In contrast, the abundances of AOA that ranged from 10^3 to 10^4 copies per mL were almost two orders of magnitude higher than those of AOB below the depth of 75 m. AOA is the dominant ammonia oxidizing

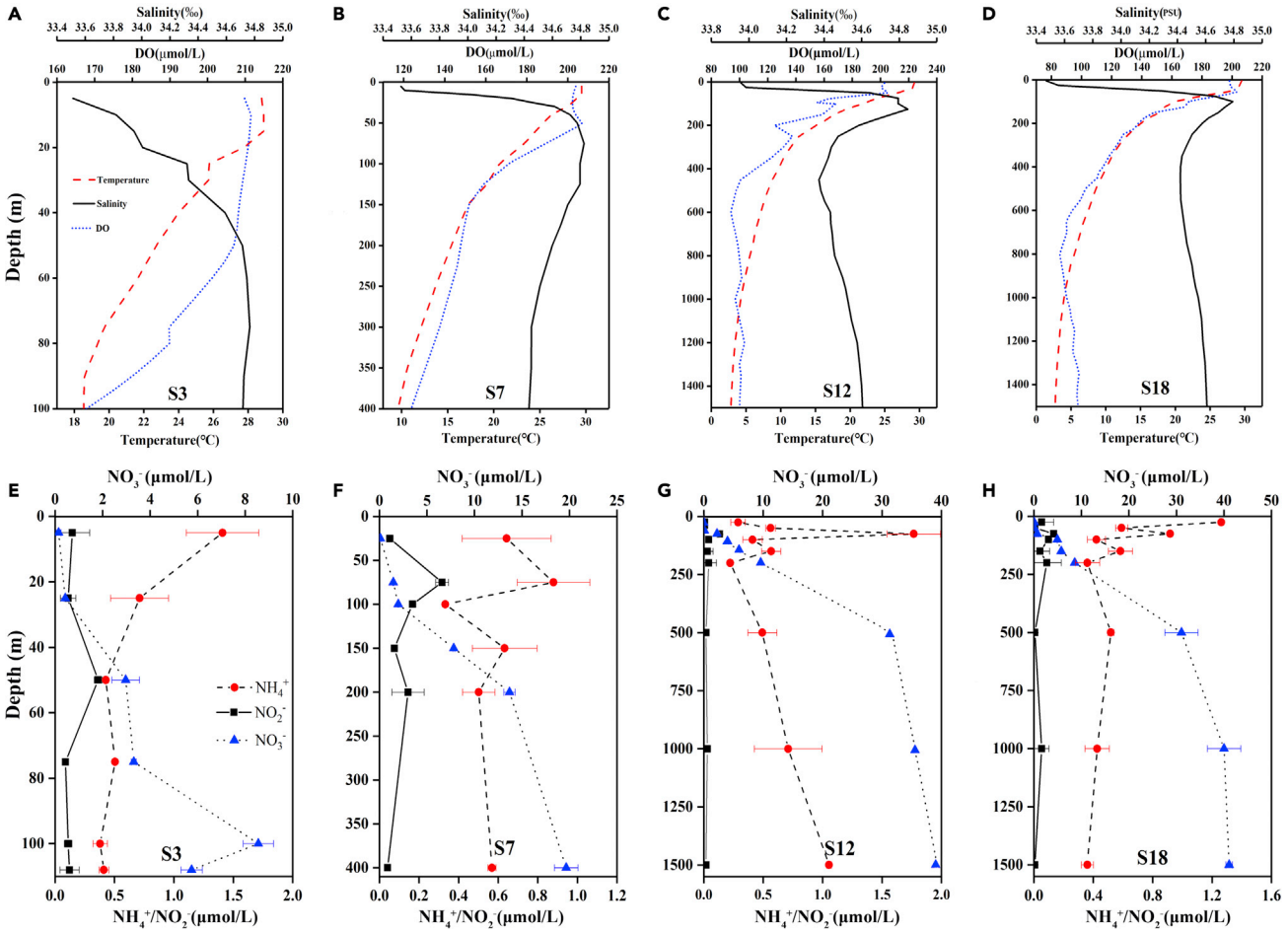

Figure 2. Depth profiles of salinity, temperature, and DO along the water columns in S3 (A), S7 (B), S12 (C), and S18 (D) in the South China Sea

Depth profiles of dissolved nitrogen contents, including NH_4^+ (red dotted lines), NO_3^-(blue triangle lines), and NO_2^-(black square lines), along the water columns in S3 (E), S7 (F), S12 (G), and S18 (H). Error bars represent the SD of triplicate reactions.

group in the deeper layers. In addition, the highest ratios of AOA/AOB were found in depths that ranged from 75 to 200 m. The highest abundances of AOA were observed at depths of 150 m or 200 m. The abundances of AOA decreased when depth below 200 m.

A total of 110,000 AOA *amoA* raw sequences (5,000 sequences per sample) were run for denoising and trimming. Approximately 4,000 reads per sample (90,877 sequences) of AOA *amoA* sequences were filtered as high-quality reads (Table 1). Seven samples, including S3-5 m, S7-25 m, S12-25 m, S12-50 m, S18-25 m, S18-50m, and S18-75 m, could not be amplified by AOA *amoA* gene-targeted PCR owing to the low abundances of AOA. Twenty-two samples generated approximately 31 operational taxonomic units (OTUs) for the AOA *amoA* gene with a Good's coverage of 0.99 at 89% similarity, providing information that the OTUs of each AOA library had been captured effectively (Figure S1). The highest number of OTUs (the average number of OTU is 24) were observed in the depth of 150 and 200 m. S3 station is the exception; the highest OTU number was found in 100 m depth. The lowest OTU number (the average number of OTU is 16) was found in sample S7-75 m and S18-100 m. Chao1 and ACE indexes, the two key estimators for calculating the community richness, ranged from 17.50 to 33.50 and 19.56 to 37.26, respectively. The Simpson and Shannon diversity indexes ranged from 0.19 to 0.51 and 0.78 to 1.91, respectively. The higher values of Shannon index were observed in depth of 200 m, whereas the lower values were found in surface layers (including 0–100 m depths). In line with the distribution of Shannon index, the lower value of Simpson index was observed in 200 m depth. Evenness of AOA *amoA* gene was low, ranging from 0.27 to 0.62, suggesting that the community composition of AOA remained relatively uneven.

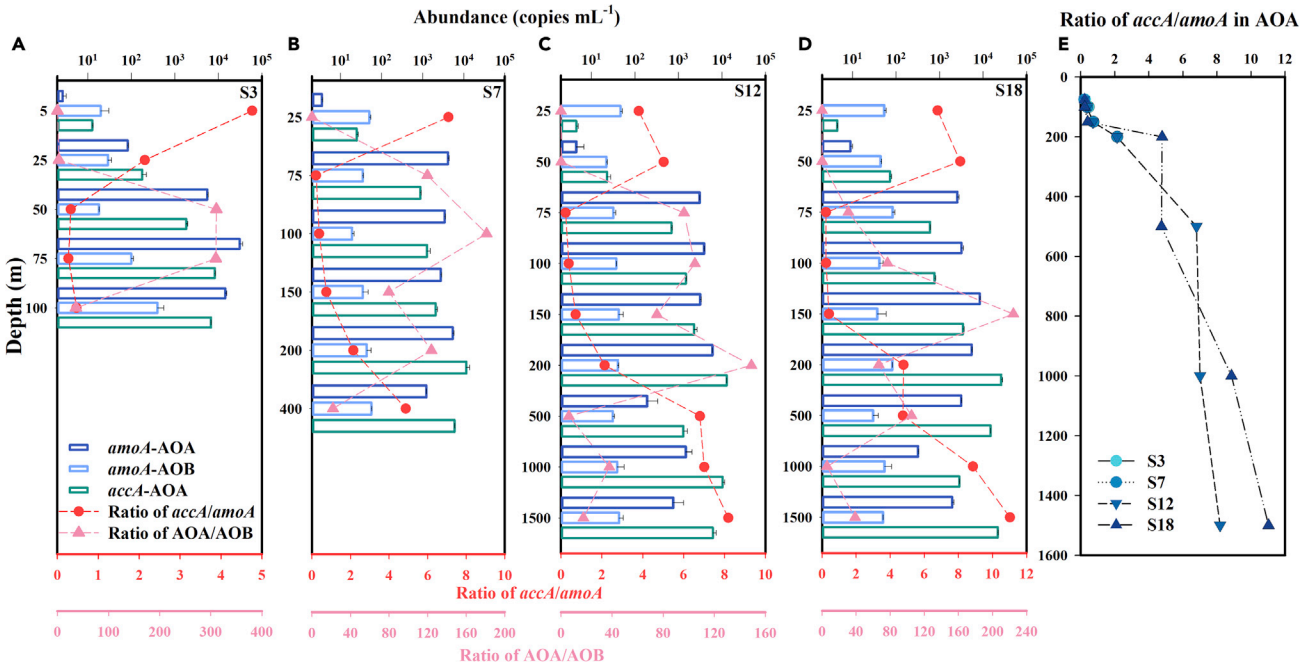

Figure 3. Depth profiles of *amoA* abundances (for AOA, deep blue bars), *amoA* abundances (for AOB, light blue bars), *accA* abundances (for AOA, green bars), the ratios of *accA*/*amoA* (red dot lines), and the ratios of AOA/AOB (pink triangle lines) in S3 (A), S7 (B), S12 (C), and S18 (D)

(E) The ratios of *accA*/*amoA* gene copy numbers of AOA along water depth in the South China Sea. Error bars represent the SD of triplicate reactions.

Depth profiles of *accA* gene abundances and diversity

The abundances of *accA* gene showed a deep depth maximum, ranging from 4.47 ± 0.25 to (2.62 ± 0.21) ×10^4 copies mL^{-1} (Figure 3, green bars). The highest abundances of *accA* gene were found at a depth of 200 m, ranging from (1.15 ± 0.26) to (2.62 ± 0.21)×10^4 copies mL^{-1}. In contrast, the lowest abundances were found in the surface layers (0–50 m). A similar pattern of distribution was observed between the depth profiles of abundances of AOA *amoA* and AOA *accA* genes. The ratios of *accA*/*amoA* gene copy numbers of AOA in the depth profiles revealed a sharp increase from <1 at a depth of 75–150 m to 11.03 at a depth of 1,500 m (Figure 3E).

Approximately 95,000 AOA *accA* raw sequences (5,000 sequences per sample) were run to denoise and trim the sequences. A total of 4,700 reads per sample (90,781 sequences) were filtered as high-quality reads (Table 2). Ten samples, including S3-5 m, S3-25 m, S7-25 m, S12-25 m, S12-50 m, S12-75 m, S18-25 m, S18-50m, S18-75 m, and S18-100 m, could not be amplified by AOA *accA* gene-targeted PCR owing to low abundances of *accA* gene. Nineteen samples generated approximately 23 OTUs for the AOA *accA* gene with a Good's coverage of 0.99 at 82% similarity, providing information that the OTUs of each *accA* gene library had been captured effectively (Figure S2). The average number of OTUs was 24, but the highest numbers of them were observed at depths of 150 and 200 m. The highest number of OTUs (22) was observed at a depth of 75 m in the S3 station, whereas the lowest number of OTUs (10) was found at a depth of 500 m in the S18 station. A significant difference of the OTU number was revealed between epipelagic (<150 m) and bathypelagic water ($p < 0.01$, $n = 10$, one-way ANOVA). The Chao1 and ACE indexes for the AOA *accA* gene ranged from 10.00 to 26.25 and 10.00 to 30.17, respectively. The Simpson and Shannon diversity indexes ranged from 0.12 to 0.97 and 0.78 to 1.54, respectively. The higher values of Shannon index and the lower values of Simpson index were found at depths of 100 and 150 m, whereas lower diversity and richness of *accA* gene were observed at depths >400 m. Consistent with the result of AOA *amoA* gene, the evenness of AOA *accA* gene was also low, ranging from 0.05 to 0.57, suggesting that the community composition of *accA* gene remained relatively uneven.

Community composition and phylogenetic analysis of the *amoA* gene

A newly developed database of AOA *amoA* was used to taxonomically classify high-quality sequences. The relative abundance of AOA *amoA* reads from the water column classified at the genus level were shown in

Table 1. The alpha diversity indexes of *amoA* gene at different depth in the South China Sea

Station	Depth	High-quality sequences*	OTUs	Coverage	Shannon	Simpson	Chao1	Ace	Evenness**
S3	25	4797	17	99.92%	0.83	0.49	32.00	20.15	0.29
S3	50	4274	18	99.86%	0.78	0.51	27.25	23.26	0.27
S3	75	3726	20	99.84%	0.92	0.47	28.75	25.67	0.31
S3	100	3591	25	99.86%	1.19	0.40	27.00	27.97	0.37
S7	75	4312	16	99.88%	0.78	0.49	26.25	19.91	0.28
S7	100	4321	18	99.93%	0.86	0.50	18.50	19.56	0.30
S7	150	3844	24	99.87%	1.44	0.35	25.00	27.10	0.45
S7	200	3906	25	99.90%	1.83	0.21	17.50	28.37	0.57
S7	400	4625	20	99.91%	1.38	0.33	28.00	22.23	0.46
S12	75	4287	17	99.86%	0.80	0.49	21.00	22.34	0.28
S12	100	3927	22	99.82%	0.87	0.48	33.50	28.75	0.28
S12	150	3872	25	99.85%	1.39	0.37	20.50	30.45	0.43
S12	200	3872	26	99.92%	1.91	0.19	20.50	27.32	0.59
S12	500	4417	21	99.84%	1.35	0.34	18.50	27.07	0.44
S12	1000	4246	17	99.91%	1.21	0.36	33.00	25.10	0.43
S12	1500	4106	18	99.83%	1.12	0.40	25.00	28.37	0.39
S18	100	4079	16	99.90%	0.84	0.48	27.00	20.06	0.30
S18	150	3762	25	99.84%	1.41	0.33	19.33	30.46	0.44
S18	200	3920	21	100.00%	1.87	0.20	18.75	21.00	0.62
S18	500	4367	23	99.84%	1.32	0.35	27.33	37.26	0.42
S18	1000	4433	18	99.89%	1.22	0.34	26.20	21.67	0.42
S18	1500	4193	19	99.90%	1.18	0.38	21.50	22.27	0.40

Note: *Trimmed reads that passed quality control; **evenness was calculated by dividing Shannon index by Ln(OTUs). The estimated richness and diversity indices were calculated at 89% similarity level.

Figure 4A. A significant shift in the community composition of AOA across water depth was observed. The surface community assemblage (<100 m depth) was primarily affiliated with *Nitrosopelagicus*. In contrast, 95% of the AOA community in the mesopelagic and bathypelagic water was closely related to uncultured sequences. A shift from *Nitrosopelagicus* to an uncultured community was found at a transitional zone between 150 and 200 m. The relative abundance of *Nitrosopelagicus* decreased with water depth. Only 3.3% of the high-quality sequences were related to unclassified sequences.

To clearly delineate the distribution of AOA community in seawater columns, seven predominant OTUs (TOP7) of AOA were selected to construct a phylogenetic tree (Figures 4B and S3). The dominant OTUs of AOA in the collected samples were phylogenetically affiliated with two different clusters. OTU01 (28.93%), OTU02 (25.51%), and OTU07 (2.42%) were members of one cluster (cluster 1), whereas OTU03 (18.05%), OTU04 (14.63%), OTU05 (6.07%), and OTU06 (2.55%) were related to another cluster (cluster 2). Clusters 1 and 2 were all affiliated with thaumarchaeal group I.1a (the marine clade). OTU01 and OTU02, which had highest relative abundance, were affiliated with *Nitrosopelagicus*. The sequences of OTU02 and *Candidatus* Nitrosopelagicus brevis CN25 (CP007026) were 99% similar. OTU07 was related to an uncultured AOA sequence from 200 m in the East China Sea (GU181727). Cluster 1 is a member of the shallow marine clade. In contrast, OTU03, OTU06, OTU05, and OTU04 were affiliated with the uncultured AOA sequences in mesopelagic and bathypelagic water (800 m and 3,000 m, respectively). The archaea in Cluster two are members of the deep marine clade.

An obvious vertical distribution of the AOA community composition was revealed by a Principal Coordinate Analysis (PCoA, Figure 4C). The first and second principal coordinates explained 57.95% and 9.48% of the variance in the AOA community composition among all the samples, respectively. Four distinct assemblages of AOA were identified. Nine samples from the 25 to 100 m depths clustered to form one group. Three samples from 150 m and another three samples from 200 m clustered to form a group, respectively.

Table 2. The alpha diversity indexes of *accA* gene at different depth in the South China Sea

Station	Depth	High-quality sequences*	OTUs	Coverage	Shannon	Simpson	Chao1	Ace	Evenness**
S3	50	4678	20	99.94%	0.81	0.69	21.50	21.84	0.27
S3	75	4740	22	99.85%	1.41	0.30	26.25	30.17	0.46
S3	100	4731	17	99.92%	1.46	0.28	22.71	23.18	0.51
S7	75	4813	19	99.92%	0.45	0.84	21.95	22.33	0.15
S7	100	4806	17	99.96%	0.98	0.58	17.40	18.15	0.34
S7	150	4750	12	100.00%	0.98	0.55	12.00	12.00	0.39
S7	200	4782	13	99.98%	0.46	0.83	13.03	13.60	0.18
S7	400	4849	11	99.96%	0.16	0.95	11.57	14.39	0.07
S12	100	4744	12	99.98%	1.33	0.33	12.02	12.64	0.54
S12	150	4765	15	99.94%	1.30	0.38	16.06	19.40	0.48
S12	200	4784	12	99.94%	0.32	0.89	14.74	18.78	0.13
S12	500	4843	11	99.98%	0.12	0.97	11.02	11.43	0.05
S12	1000	4759	13	99.94%	0.16	0.95	14.53	15.33	0.06
S12	1500	4758	12	99.98%	0.17	0.95	11.98	12.40	0.07
S18	150	4800	15	99.96%	1.54	0.25	15.78	16.30	0.57
S18	200	4802	11	99.98%	0.34	0.88	10.98	11.39	0.14
S18	500	4863	10	100.00%	0.17	0.95	10.00	10.00	0.07
S18	1000	4763	12	99.96%	0.16	0.95	12.88	13.56	0.06
S18	1500	4751	11	100.00%	0.19	0.94	11.00	11.00	0.08

Note: *Trimmed reads that passed quality control; **evenness was calculated by dividing Shannon index by Ln(OTUs). The estimated richness and diversity indices were calculated at 82% similarity level.

The remaining samples from mesopelagic and bathypelagic water (>400 m) were the final group. Figure 4D shows a heatmap analysis of seven selected dominant OTUs across all the samples. OTU01 and OTU02 were primarily distributed in the epipelagic water (<200 m). In contrast, OTU03, OTU04, and OTU05 were primarily distributed in the mesopelagic and bathypelagic water with depths >400 m. In addition, OTU06 and OTU07 dominated the AOA community composition in the depths between 150 and 200 m. All the dominant OTUs were cosmopolitan and commonly present in the depth between 150 and 200 m. A redundancy analysis (RDA) with the dominant OTUs showed that the first two axes (RDA1 and RDA2) explained 92.10% of the cumulative variance in the AOA communities (Figure S5). Depth ($F = 15.5$. $p = 0.014$; RDA) and temperature ($F = 50.6$. $p = 0.014$; RDA) were the key factors that influenced the community composition of AOA. In addition, these two factors accounted for 84.4% of the total variation.

Community composition and phylogenetic analysis of the *accA* gene

A phylogenetic tree was constructed using the dominant 14 OTUs and reference sequences for *accA* gene (Figure 5A). The dominant OTUs of *accA* gene in the collected samples were phylogenetically affiliated with two different clusters, which was consistent with the result of AOA *amoA* gene. OTU01 (64.67%) and OTU06 (0.63%) were members of one cluster (cluster 1), whereas the remaining OTUs were members of another cluster (cluster 2). The sequences of OTU02 and *Candidatus* Nitrosopelagicus brevis CN25 (CP007026) were 94% similar. The sequence of OTU07 was similar to that of *N. maritimus* SCM1 (CP000866). The features of cluster 1, including OTU02, OTU03, OTU04, OTU09, OTU05, OTU14, OTU08, OTU12, and OTU07, indicated that they were closely related to the environmental sequences (GU195401, GU195464, and KC349333) from the surface seawater (<100 m) and are members of the shallow marine clade. Cluster 2, including OTU06 and OTU01, was related to an uncultured *accA* sequence in 400 m deep seawater from the East China Sea (GU195578). OTU11, OTU10, and OTU13 were not related to any known uncultured sequence and are members of the unknown cluster.

Similarly, the PCoA analysis based on *accA* gene revealed a significant vertical distribution of the community composition of AOA (Figure 5B). The first and second principal coordinates explained 67.02% and 10.89% of the variance in the community composition among all the samples, respectively. Four distinct

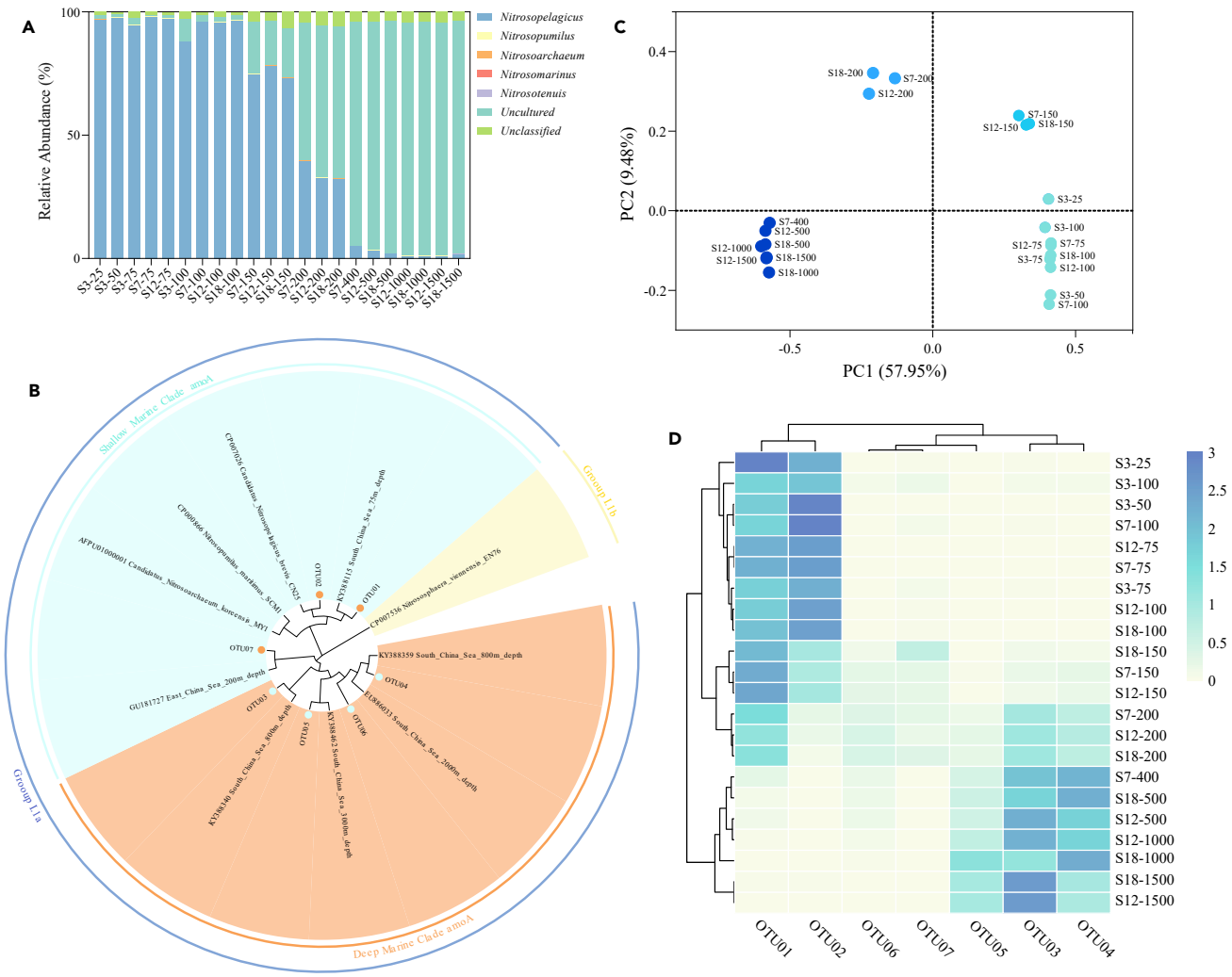

Figure 4. Microbial characteristics of the AOA *amoA* gene along the water depth in the SCS

(A) AOA community compositions at different depths of four stations. Relative abundance of AOA *amoA* reads from the water column classified at the genus level. Reads were classified in the template databases by using a confidence threshold of 80%. Uncultured reads were affiliated with uncultured Thaumarchaeota. Unclassified reads represent no matching sequence in the template database.

(B) Phylogenetic tree of the dominant OTUs (number of sequences >1% of total sequences) in the South China Sea. Neighbor-joining tree was constructed from AOA *amoA* gene amplicon sequencing and bootstrap analysis with 1000 replicates used to estimate confidence. Bootstrap values of >50% were listed in the tree.

(C) Principal coordinates analysis (PCoA) of AOA communities in the water column of four stations based on OTU. Percentages on the axes of the graph represent the explained variance of total variance. The OTU data matrix used in the analyses was clustered at the 89% similarity, and the principal coordinates analysis was based on the thetayc model. Each point corresponds to a sample.

(D) The heatmap of the most abundant *amoA* OTUs (top seven OTUs, 89% cutoff).

assemblages of AOA *accA* gene were found. Ten samples from mesopelagic and bathypelagic water (>200 m) were clustered to form one group, which were distinct from the communities of other three surface groups (50–150 m). A heatmap analysis of four selected dominant OTUs across all the samples is shown in Figure 5C. OTU01, a member of the deep marine clade, was primarily distributed in mesopelagic and bathypelagic water (>200 m). The remaining OTUs, including OTU02, OTU03, and OTU04, were members of the shallow marine clade and primarily distributed in epipelagic water (<200 m). All the dominant OTUs are cosmopolitan and commonly present in the depths between 100 and 150 m. An RDA with the dominant OTUs of *accA* gene showed that the first two axes (RDA1 and RDA2) explained 89.39% of the cumulative variance (Figure S6). The amount of DO ($F = 43.7$, $p = 0.02$; RDA) and contents of NO_3^- ($F = 4.7$,

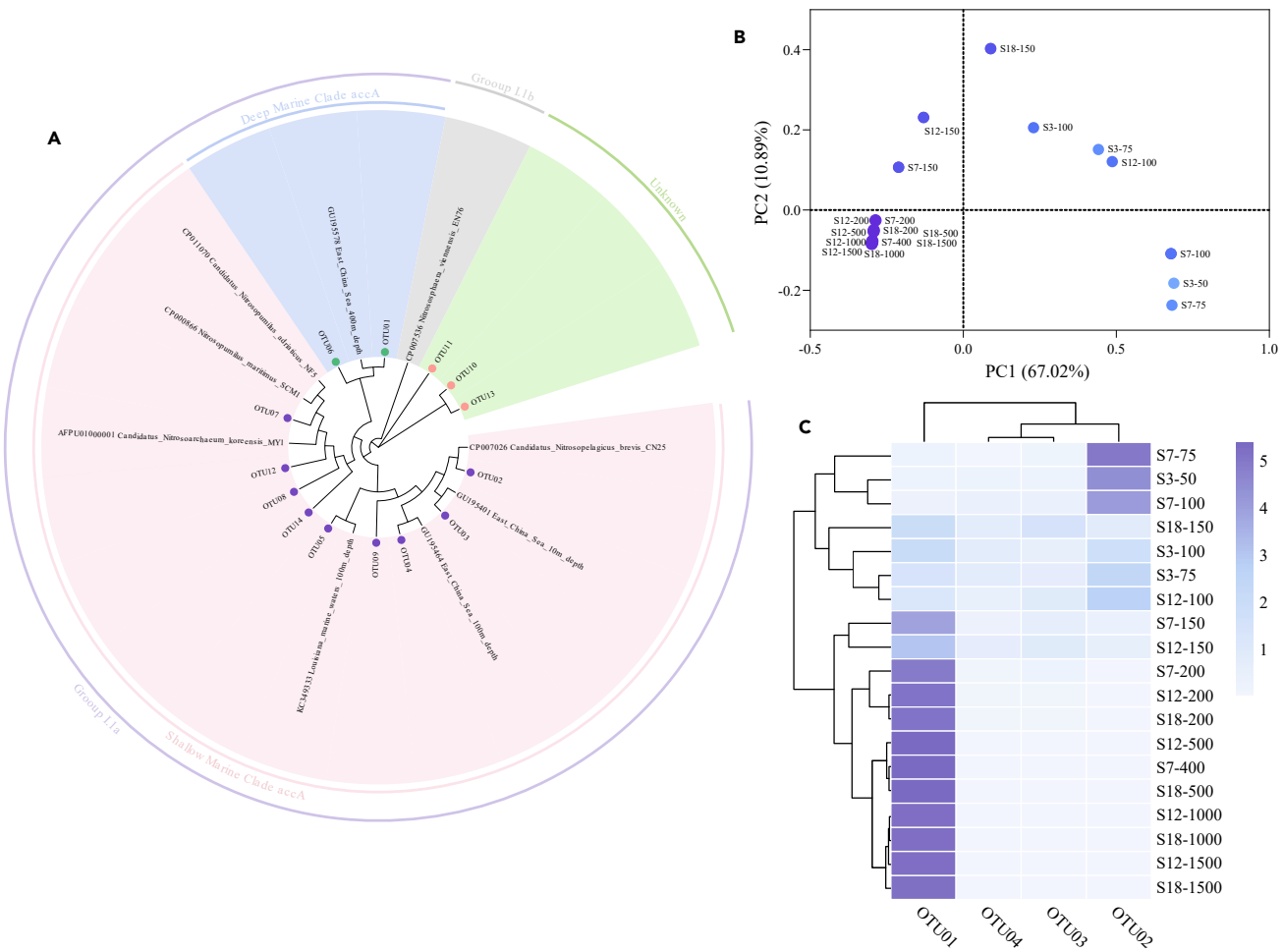

Figure 5. Microbial characteristics of the AOA *accA* gene along the water depth in the SCS

(A) Phylogenetic tree of the dominant OTUs (number of sequences >50) in the South China Sea. Neighbor-joining tree was constructed from *accA* gene amplicon sequencing and bootstrap analysis with 1000 replicates used to estimate confidence. Bootstrap values of >50% were listed in the tree.

(B) Principal coordinates analysis (PCoA) of *accA* gene in depth profiles at four stations in the South China Sea based on OTU. The community structures were analyzed by PCoA based on thetayc distance matrix. PC1 and PC2 are shown with the percentage variation explained for each axis.

(C) The heatmap of the most abundant *accA* OTUs (top four OTUs, 82% cutoff).

p = 0.012; RDA) were the key factors that influenced the community composition of *accA* gene. In addition, these two factors accounted for 78.32% of the total variation.

DISCUSSION

Distribution and carbon fixation potential of AOA in the epipelagic zone

AOA are among the most abundant and ubiquitous microorganisms, which play key roles in nitrification and the emission of nitrous oxides from the ocean (Qin et al., 2020). Their distribution and diversity in different ecosystems have been investigated by increasing numbers of studies (Francis et al., 2005; Gubry-Rangin et al., 2011; Hou et al., 2018; Yang et al., 2021; Zhang et al., 2008). However, knowledge on the vertical distribution of AOA community in seawater columns was limited. In this study, the depth profiles of AOP abundances are shown in Figures 3A–3D. The abundances of AOA *amoA* gene fall within the ranges reported in the water column of the SCS (Zhang et al., 2020) and coastal waters of Antarctica (Tolar et al., 2013). The abundances of AOP were relatively lower in the depths between 0 and 50 m that have a high intensity of light. In addition, lower diversity of AOA was also observed at depths of 25–100 m. As shown in previous studies, light has long been implicated as a major factor affecting the activity and decreases the abundances of AOP and nitrite oxidizers in the water column (Merbt et al., 2012; Xu et al.,

2019). The photoinhibition on cultured AOB attributed to photooxidative damage of the copper-containing ammonia monooxygenase. But the mechanism of photoinhibition has not yet been determined for AOA (Hooper and Terry, 1974; Hyman and Arp, 1992; Lu et al., 2020). Thus, high light intensity in the upper layer resulted in lower AOP abundances in this study. However, the intensity of light was gradually attenuated as the depth of water increased. Thus, the light inhibition of AOA was gradually eliminated, resulting an increase in the abundance of AOA. The highest abundance of AOA was found at the depths between 75 and 200 m (Figures 3B–3D) that had the highest concentration of NH_4^+ (Figures 2F–2H). In addition, the AOA were highly diverse at the bottom of euphotic zone (from 150 to 200 m), which had the maximum quantity of OTU (average 23). The increase in NH_4^+, which is transported from the mineralization of organic matter in the surface water, can serve as the available substrate for ammonia oxidation and support higher abundances in AOA in the depths between 75 and 200 m. Based on the AOA sequences (Figure 4A) and dominant OTU annotation (Figures 4C and 4D), a significant vertical distribution of the AOA community was observed, and the surface assemblage of AOA was primarily affiliated with *Nitrosopelagicus*. *Candidatus* Nitrosopelagicus brevis is primarily distributed in the upper ocean and is a model species of AOA (Santoro and Casciotti, 2011; Santoro et al., 2015). Santoro et al. (2015) found that *Ca. N. brevis* has unique proteins that can adapt to the oligotrophic conditions in the upper ocean.

accA gene is the key gene that encodes the acetyl-CoA carboxylase α-submit of autotrophic carbon fixation in AOA, which is usually used as the index to evaluate the autotrophic potential (Bergauer et al., 2013; Hu et al., 2011a, 2011b; Song et al., 2013; Yakimov et al., 2009, 2011). In this study, *accA* gene was detected in all the water layers, including the epi-, meso-, and bathypelagic zones (Figure 5A). However, a lower abundance of *accA* gene and the ratio of *accA* and *amoA* gene (<1) was detected in the surface water with depths lower than 50 m, suggesting the lower autotrophic potential of AOA in the surface layers. AOA may rely on heterotrophy and play a minor role in carbon fixation in epipelagic water with higher organic matter (Hu et al., 2011a, 2011b). Two carbon fixation pathways, 3-HP/4-HB and the oxidative tricarboxylic acid (TCA) cycles, coexist in *Cenarchaeum symbiosum A*, which suggests that it can obtain energy from autotrophic and heterotrophic metabolism (Hallam et al., 2006). Thus, AOA can obtain energy from heterotrophic and autotrophic metabolism in the euphotic zone. Furthermore, the diversity and community composition of *accA* gene at the depths of 5–75 m were not detected owing to the lower abundances of *accA* gene (Figure 5 and Table 2). A significant vertical distribution of *accA* gene was also observed, which is consistent with the pattern of distribution of *amoA* gene. A shallow cluster of dominant OTU (primarily OTU02) was distributed at 50 to 150 m and is closely related to *Candidatus* Nitrosopelagicus brevis CN25 (CP007026).

Distribution and carbon fixation potential of AOA in the mesopelagic and bathypelagic zones

In contrast to the lower abundance and diversity of AOA in epipelagic water, higher abundance and diversity were observed below the surface layers (Figures 3B–3D). In contrast, owing to the lower contents of NH_4^+ at depths below 200 m (Figures 2F–2H), the abundance of AOA tended to decrease (Figures 3B–3D). Based on the AOA sequences (Figure 4A) and annotation of dominant OTUs (Figures 4C and 4D), the deep assemblage of AOA was closely related to uncultured sequences and the deep marine clade that is part of thaumarchaeal group I.1a (the marine clade). A PCoA analysis also showed that samples collected from depths of 400, 500, 1,000, and 1,500 m clustered together (Figure 4C). It is primarily because enriched or pure cultures of AOA in the deep sea were not available to serve as a reference sequence. A significant vertical distribution of the AOA community in seawater column was driven by light inhibition, which is consistent with research from the SCS (Hu et al., 2011a) and Tyrrhenian Sea (Yakimov et al., 2009, 2011). An RDA analysis showed that the depth and temperature significantly influenced the AOA community in the seawater columns of the SCS (Figure S5). Seawater stratification along the depths may result in the niche differences of AOA.

A higher abundance of *accA* gene (average 1.69×10^4 copies mL^{-1}) was found at 200 m, suggesting a higher autotrophic potential of AOA in the deep water, particularly at the bottom of the euphotic zone. The ratios of *accA* and *amoA* gene increased with the water depth to reach 11.03 at 1,500 m (Figure 3E). The ability of the uncultured AOA found in the deep and oligotrophic water to oxidize NH_4^+ to support autotrophic growth was proposed as an explanation for the higher numbers of *accA* gene in deep water (Hu et al., 2011a, 2011b). The difference in organic matter between the surface and deep water may result in significant vertical distribution of *accA* gene. The organic matter demand of AOA in the deep water was higher than that in the surface water. The deep cluster utilizes an autotrophic carbon fixation process to obtain

carbon, whereas the shallow cluster uses heterotrophic or mixotrophic metabolism to use the organic matter from phytoplankton in the surface water that sinks to the lower levels. The OTU of shallow cluster gradually shifts to the OTU of deep cluster as the depth of seawater increases, which is consistent with the findings from the SCS (Hu et al., 2011a, 2011b). The vertical succession of the AOA community compositions was observed by the heatmap analysis of *amoA* (Figure 4D) and *accA* genes (Figure 5C). The dominant OTU of the deep marine clade was distributed between 150 and 1,500 m.

The ecological significance of autotrophic carbon fixation for AOA in the deep dark ocean

Oceans play a significant role in absorbing CO_2 from the atmosphere and storing it in the deep sediment (Jiao et al., 2010; Zhang et al., 2020). As one of significant sinks of atmospheric CO_2 in the earth, the ocean has an important role in regulating the global carbon cycle and climate change. Typically, the photosynthetic process driven by phytoplankton generates approximately 30–50 Gt $year^{-1}$ of organic matter in the euphotic zone, which is an important source of organic matter in the ocean (Antoine et al., 1996). Most of the marine POM that sinks from the euphotic zone will be rapidly mineralized by prokaryotic microorganisms and generate energy (del Giorgio and Duarte, 2002). Thus, approximately 10% of the primary productivity in the euphotic zone can reach 200 m, whereas only 1% of POM can reach the seabed and be buried (Suess, 1980). The traditional view is that carbon fixation in the ocean primarily depends on the photosynthesis of phytoplankton, whereas the carbon fixation in the dark ocean is usually ignored. Nevertheless, the dark ocean is the largest biosphere on earth, with a volume of 1.3×10^{18} m^3. Increasing evidence shows that the dark ocean is an active food web layer and plays an important role in the cycle of material and energy flow of the whole water column. Based on the Redfield ratio (C:N = 16:1) (Redfield et al., 1963), an enormous amount of NH_4^+ will be generated by the mineralization of sinking POM from the euphotic zone. Furthermore, higher abundances of AOA that ranged from 10^3 to 10^4 copies mL^{-1} were observed in the meso- and bathypelagic zones (Figures 3A–3D). In addition, a higher potential of carbon fixation was apparent in the deep dark ocean by the higher abundances of *accA* gene of the AOA and the increasing pattern of ratios of *accA*/*amoA* gene (Figure 3). The NH_4^+ will be transformed to NO_3^- by the microbial nitrification process of AOA and stored in the ocean. In the interim, the chemical energy stored in NH_4^+ will be obtained by microorganisms and used for carbon fixation and the synthesis of organic matter. For example, AOA, the most abundant ammonia oxidizers in the deep dark ocean, fix carbon by consuming ATP through the 3-HP/4-HB cycle with the key enzyme encoded by *accA* gene. The water column in global ocean has a high amount of oxygen. Such high DO conditions favor the microbial process of the oxidation of ammonia under aerobic conditions and also limit anaerobic respiration by microorganisms. Therefore, from the theoretical analysis of flux estimation and high DO conditions, the microbial ammonia oxidation driven by AOA should be an important energy source in the deep dark ocean. It is well known that the oxidation of ammonia to nitrite requires oxygen. However, AOA are even highly abundant in environments with low oxygen concentration, such as the marine oxygen minimum zones (OMZs, < 1% of the global ocean water volume) (Berg et al., 2015; Lam and Kuypers, 2011; Stewart et al., 2012). More recently, Kraft et al. (2022) found that the marine AOA *N. maritimus* produces dinitrogen and oxygen for ammonia oxidation in the dark and low oxygen condition. These results suggest that autotrophic carbon fixation by AOA in the strictly anoxic OMZs is also an important contributor to the ocean carbon budget.

Compared with the photosynthesis of phytoplankton in the euphotic zone (30–50 Gt yr^{-1} (Hedges et al., 1997), the carbon fixation flux of the autotrophic process (0.6–0.7 Gt C yr^{-1}, Ingalls et al., 2006) is much lower. However, it has provided "new" organic carbon into the deep ocean, which is an important contributor to the ocean carbon budget and affects the food web structure. In addition, the fixation of autotrophic carbon by AOA may degrade the sinking POM to refractory carbon and bury it in the deep-sea sediment for a long time. In this way, carbon dioxide in the ocean does not have to be recycled back to the atmosphere on the millennium timescale, and this part of carbon may be "isolated" for a longer timescale. Therefore, autotrophic carbon fixation by the ammonia oxidation process of AOA should be an important contributor to the marine microbial carbon pump (Jiao et al., 2010).

Conclusions

This study highlights the depth-related shift of community compositions and the potential of AOA communities in water columns of the South China Sea to autotrophically fix carbon. AOA, not AOB, have the dominant role in the process of oxidizing ammonia in the deep seawater column in the SCS, which is primarily distributed below 75 m. The AOA in epipelagic water were closely related to *Nitrosopelagicus*, whereas the

deep assemblage of AOA was affiliated with unclassified sequences. However, all the sequences of AOA belong to thaumarchaeal group I.1a (the marine clade). Interestingly, vertical niche differences along the water depth were shown by the community compositions and abundances of *amoA* and *accA* genes in this study. Vertical profiles of organic matter and light intensity affect the distribution of AOA in deep sea water. A higher potential to autotrophically fix carbon, as indicated by the ratios of *accA* and *amoA* genes, was found in the deep water. AOA can obtain energy from heterotrophic and autotrophic metabolism in the upper ocean that has more available and sufficient levels of organic carbon. In contrast, AOA oxidize ammonia to support autotrophic growth in the deep and oligotrophic water. Overall, this study provides information on the potential of niche-segregated AOA communities to fix carbon autotrophically in the water columns of the SCS.

Limitations of the study

In this study, the carbon fixation potential of AOA was identified by the ratios of *accA* and *amoA* genes. The rate and flux of carbon fixation of AOA in water columns of the SCS are not known. The rates of ammonia oxidation and fixation of dissolved inorganic carbon, measured using $^{15}NH_4^+$ and $^{13}C\text{-}HCO_3^-$ as the tracers, will be employed in future research.

STAR★METHODS

Detailed methods are provided in the online version of this paper and include the following:

- KEY RESOURCES TABLE
- RESOURCE AVAILABILITY
  - Lead contact
  - Material availability
  - Data and code availability
- METHOD DETAILS
  - Sample collection and physicochemical parameters determination
  - DNA extraction and qPCR assay of *amoA* and *accA* genes
  - PCR amplification and high-throughput sequencing analysis
- QUANTIFICATION AND STATISTICAL ANALYSIS
  - Statistical analysis

SUPPLEMENTAL INFORMATION

Supplemental information can be found online at https://doi.org/10.1016/j.isci.2022.104333.

ACKNOWLEDGMENTS

We would like to thank the grants financially supported by the National Natural Science Foundation of China (No. 42006122, No. 91851111 and No. 31870100), Natural Science Foundation of Guangdong Province (No. 2021A1515011548), Basic and Applied Basic Research Foundation of Guangdong Province (No. 2020A1515110597 and No. 2019B1515120066), Science and Technology Projects in Guangzhou (No. 202102021232 and No. 202102010460), and Young Talent Research Project of Guangzhou Education Bureau (No. 202032795).

AUTHOR CONTRIBUTIONS

J.W., X.H., and Y.H. performed research; J.W., X.H., X.L., J.Y., L.J., Y.L., Y.W. Y.Y., and J.D. analyzed data; J.W. and Y.H wrote the paper, and all co-authors substantially contributed to comments and revisions. All authors read and approved the final manuscript.

DECLARATION OF INTERESTS

The authors declare no competing interests.

Received: January 18, 2022
Revised: April 12, 2022
Accepted: April 26, 2022
Published: May 20, 2022

REFERENCES

Antoine, D., André, J.-M., and Morel, A. (1996). Oceanic primary production: 2. Estimation at global scale from satellite (Coastal Zone Color Scanner) chlorophyll. Glob. Biogeochem. Cycles *10*, 57–69. https://doi.org/10.1029/95gb02832.

Baltar, F., Arístegui, J., Gasol, J.M., Sintes, E., and Herndl, G.J. (2009). Evidence of prokaryotic metabolism on suspended particulate organic matter in the dark waters of the subtropical North Atlantic. Limnol. Oceanogr. *54*, 182–193. https://doi.org/10.4319/lo.2009.54.1.0182.

Berg, C., Vandieken, V., Thamdrup, B., and Jürgens, K. (2015). Significance of archaeal nitrification in hypoxic waters of the Baltic Sea. ISME J. *9*, 1319–1332. https://doi.org/10.1038/ismej.2014.218.

Bergauer, K., Sintes, E., van Bleijswijk, J., Witte, H., and Herndl, G.J. (2013). Abundance and distribution of archaeal acetyl-CoA/propionyl-CoA carboxylase genes indicative for putatively chemoautotrophic Archaea in the tropical Atlantic's interior. FEMS Microbiol. Ecol. *84*, 461–473. https://doi.org/10.1111/1574-6941.12073.

Blainey, P.C., Mosier, A.C., Potanina, A., Francis, C.A., and Quake, S.R. (2011). Genome of a low-salinity ammonia-oxidizing archaeon determined by single-cell and metagenomic analysis. PLoS One *6*, e16626. https://doi.org/10.1371/journal.pone.0016626.

Carlson, C.A., Ducklow, H.W., and Michaels, A.F. (1994). Annual flux of dissolved organic carbon from the euphotic zone in the northwestern Sargasso Sea. Nature *371*, 405–408. https://doi.org/10.1038/371405a0.

Chain, P., Lamerdin, J., Larimer, F., Regala, W., Lao, V., Land, M., Hauser, L., Hooper, A., Klotz, M., Norton, J., et al. (2003). Complete genome sequence of the ammonia-oxidizing bacterium and obligate chemolithoautotroph *Nitrosomonas europaea*. J. Bacteriol. *185*, 2759–2773. https://doi.org/10.1128/jb.185.21.6496.2003.

Chakraborty, P., Mason, R.P., Jayachandran, S., Vudamala, K., Armoury, K., Sarkar, A., Chakraborty, S., Bardhan, P., and Naik, R. (2016). Effects of bottom water oxygen concentrations on mercury distribution and speciation in sediments below the oxygen minimum zone of the Arabian Sea. Mar. Chem. *186*, 24–32. https://doi.org/10.1016/j.marchem.2016.07.005.

del Giorgio, P.A., and Duarte, C.M. (2002). Respiration in the open ocean. Nature *420*, 379–384. https://doi.org/10.1038/nature01165.

Francis, C.A., Roberts, K.J., Beman, J.M., Santoro, A.E., and Oakley, B.B. (2005). Ubiquity and diversity of ammonia-oxidizing archaea in water columns and sediments of the ocean. Proc. Natl. Acad. Sci. U S A *102*, 14683–14688. https://doi.org/10.1073/pnas.0506625102.

Guan, F., Hong, Y., Jiapeng, W.U., Wang, Y., Liying, B., Tang, B., and Xie, G. (2017). A fast sodium hypobromite oxidation method for the sequential determination of ammonia nitrogen in small volume. Ecol. Sci. *36*, 42–48.

Gubry-Rangin, C., Hai, B., Quince, C., Engel, M., Thomson, B.C., James, P., Schloter, M., Griffiths, R.I., Prosser, J.I., and Nicol, G.W. (2011). Niche specialization of terrestrial archaeal ammonia oxidizers. Proc. Natl. Acad. Sci. U S A *108*, 21206–21211. https://doi.org/10.1073/pnas.1109000108.

Hallam, S.J., Konstantinidis, K.T., Putnam, N., Schleper, C., Watanabe, Y.-I., Sugahara, J., Preston, C., de la Torre, J., Richardson, P.M., and DeLong, E.F. (2006). Genomic analysis of the uncultivated marine crenarchaeote *Cenarchaeum symbiosum*. Proc. Natl. Acad. Sci. U S A *103*, 18296–18301. https://doi.org/10.1073/pnas.0608549103.

Hansman, R.L., Griffin, S., Watson, J.T., Druffel, E.R.M., Ingalls, A.E., Pearson, A., and Aluwihare, L.I. (2009). The radiocarbon signature of microorganisms in the mesopelagic ocean. Proc. Natl. Acad. Sci. U S A *106*, 6513–6518. https://doi.org/10.1073/pnas.0810871106.

He, X., Wu, J., Jiao, L., Wen, X., Wang, Y., Ou, L., and Hong, Y. (2018). Development of a method for ammonia-oxidizing archaea diversity analysis based on amoA gene amplicons with high-throughput sequencing. Microbiol. China *45*, 1861–1870.

He, Z., Zhang, H., Gao, S., Lercher, M.J., Chen, W.H., and Hu, S. (2016). Evolview v2: an online visualization and management tool for customized and annotated phylogenetic trees. Nucleic Acids Res. *44*, W236–W241. https://doi.org/10.1093/nar/gkw370.

Hedges, J.I., Keil, R.G., and Benner, R. (1997). What happens to terrestrial organic matter in the ocean? Org. Geochem. *27*, 195–212. https://doi.org/10.1016/s0146-6380(97)00066-1.

Herndl, G.J., Reinthaler, T., Teira, E., van Aken, H., Veth, C., Pernthaler, A., and Pernthaler, J. (2005). Contribution of *Archaea* to total prokaryotic production in the deep Atlantic Ocean. Appl. Environ. Microbiol. *71*, 2303–2309. https://doi.org/10.1128/aem.71.5.2303-2309.2005.

Hong, Y., Wu, J., Jiao, L., Hu, Y., Ye, F., Wang, Y., Li, Y., Wang, L., and Long, A. (2021). Shifts in the abundance and community composition of particle-associated and free-living Nitrospira across physicochemical gradients in the pearl river estuary. Estuaries Coasts *44*, 1931–1945.

Hooper, A.B., and Terry, K.R. (1974). Photoinactivation of ammonia oxidation in *Nitrosomonas*. J. Bacteriol. *119*, 899–906. https://doi.org/10.1128/jb.119.3.899-906.1974.

Hou, L., Xie, X., Wan, X., Kao, S.J., Jiao, N., and Zhang, Y. (2018). Niche differentiation of ammonia and nitrite oxidizers along a salinity gradient from the Pearl River estuary to the South China Sea. Biogeosciences *15*, 5169–5187. https://doi.org/10.5194/bg-15-5169-2018.

Hu, A., Jiao, N., and Zhang, C.L. (2011a). Community structure and function of planktonic crenarchaeota: changes with depth in the South China sea. Microb. Ecol. *62*, 549–563. https://doi.org/10.1007/s00248-011-9866-z.

Hu, A., Jiao, N., Zhang, R., and Yang, Z. (2011b). Niche partitioning of marine group I crenarchaeota in the euphotic and upper mesopelagic zones of the east China sea. Appl. Environ. Microbiol. *77*, 7469–7478. https://doi.org/10.1128/aem.00294-11.

Hyman, M.R., and Arp, D.J. (1992). 14C2H2- and 14CO2-labeling studies of the de novo synthesis of polypeptides by Nitrosomonas europaea during recovery from acetylene and light inactivation of ammonia monooxygenase. J. Biol. Chem. *267*, 1534–1545. https://doi.org/10.1016/s0021-9258(18)45979-0.

Ingalls, A.E., Shah, S.R., Hansman, R.L., Aluwihare, L.I., Santos, G.M., Druffel, E.R.M., and Pearson, A. (2006). Quantifying archaeal community autotrophy in the mesopelagic ocean using natural radiocarbon. Proc. Natl. Acad. Sci. U S A *103*, 6442–6447. https://doi.org/10.1073/pnas.0510157103.

Jiao, N., Herndl, G.J., Hansell, D.A., Benner, R., Kattner, G., Wilhelm, S.W., Kirchman, D.L., Weinbauer, M.G., Luo, T., Chen, F., and Azam, F. (2010). Microbial production of recalcitrant dissolved organic matter: long-term carbon storage in the global ocean. Nat. Rev. Microbiol. *8*, 593–599. https://doi.org/10.1038/nrmicro2386.

Könneke, M., Schubert, D.M., Brown, P.C., Hügler, M., Standfest, S., Schwander, T., Schada von Borzyskowski, L., Erb, T.J., Stahl, D.A., and Berg, I.A. (2014). Ammonia-oxidizing archaea use the most energy-efficient aerobic pathway for CO_2 fixation. Proc. Natl. Acad. Sci. U S A *111*, 8239–8244. https://doi.org/10.1073/pnas.1402028111.

Karl, D.M., Knauer, G.A., Martin, J.H., and Ward, B.B. (1984). Bacterial chemolithotrophy in the ocean is associated with sinking particles. Nature *309*, 54–56. https://doi.org/10.1038/309054a0.

Kelly, D.P. (1978). Bioenergetics of Chemolithotrophic Bacteria. Companion to microbiology (Longman), pp. 363–386.

Kraft, B., Jehmlich, N., Larsen, M., Bristow, L.A., Könneke, M., Thamdrup, B., and Canfield, D.E. (2022). Oxygen and nitrogen production by an ammonia-oxidizing archaeon. Science *375*, 97–100. https://doi.org/10.1126/science.abe6733.

Kumar, S., Stecher, G., and Tamura, K. (2016). MEGA7: Molecular Evolutionary Genetics Analysis Version 7.0 for Bigger Datasets. Molecular Biology and Evolution *33*, 1870–1874.

Lam, P., and Kuypers, M.M.M. (2011). Microbial nitrogen cycling processes in oxygen minimum zones. Annu. Rev. Mar. Sci. *3*, 317–345. https://doi.org/10.1146/annurev-marine-120709-142814.

Lu, S., Liu, X., Liu, C., Cheng, G., and Shen, H. (2020). Influence of photoinhibition on nitrification by ammonia-oxidizing microorganisms in aquatic ecosystems. Rev. Environ. Sci. Biotechnol. *19*, 531–542. https://doi.org/10.1007/s11157-020-09540-2.

Merbt, S.N., Stahl, D.A., Casamayor, E.O., Martí, E., Nicol, G.W., and Prosser, J.I. (2012). Differential photoinhibition of bacterial and archaeal ammonia oxidation. FEMS Microbiol. Lett. *327*, 41–46. https://doi.org/10.1111/j.1574-6968.2011.02457.x.

Qin, W., Zheng, Y., Zhao, F., Wang, Y., Urakawa, H., Martens-Habbena, W., Liu, H., Huang, X., Zhang, X., Nakagawa, T., et al. (2020). Alternative strategies of nutrient acquisition and energy conservation map to the biogeography of marine ammonia-oxidizing archaea. ISME J. *14*, 2595–2609. https://doi.org/10.1038/s41396-020-0710-7.

Redfield, A.C., Ketchum, B.H., and Richards, F.A. (1963). The Influence of Organisms on the Composition of Sea-Water (Interscience Publishers).

Reinthaler, T., van Aken, H., Veth, C., Arístegui, J., Robinson, C., Williams, P.J.l.B., Lebaron, P., and Herndl, G.J. (2006). Prokaryotic respiration and production in the meso- and bathypelagic realm of the eastern and western North Atlantic basin. Limnol. Oceanogr. *51*, 1262–1273. https://doi.org/10.4319/lo.2006.51.3.1262.

Reinthaler, T., van Aken, H.M., and Herndl, G.J. (2010). Major contribution of autotrophy to microbial carbon cycling in the deep North Atlantic's interior. Deep Sea Res. Part Top. Stud. Oceanogr. *57*, 1572–1580. https://doi.org/10.1016/j.dsr2.2010.02.023.

Rotthauwe, J.H., Witzel, K.P., and Liesack, W. (1997). The ammonia monooxygenase structural gene amoA as a functional marker: molecular fine-scale analysis of natural ammonia-oxidizing populations. Appl. Environ. Microbiol. *63*, 4704–4712. https://doi.org/10.1128/aem.63.12.4704-4712.1997.

Santoro, A.E., and Casciotti, K.L. (2011). Enrichment and characterization of ammonia-oxidizing archaea from the open ocean: phylogeny, physiology and stable isotope fractionation. ISME J. *5*, 1796–1808. https://doi.org/10.1038/ismej.2011.58.

Santoro, A.E., Dupont, C.L., Richter, R.A., Craig, M.T., Carini, P., McIlvin, M.R., Yang, Y., Orsi, W.D., Moran, D.M., and Saito, M.A. (2015). Genomic and proteomic characterization of "Candidatus Nitrosopelagicus brevis": an ammonia-oxidizing archaeon from the open ocean. Proc. Natl. Acad. Sci. U S A *112*, 1173–1178. https://doi.org/10.1073/pnas.1416223112.

Schloss, P.D., Westcott, S.L., Ryabin, T., Hall, J.R., Hartmann, M., Hollister, E.B., Lesniewski, R.A., Oakley, B.B., Parks, D.H., Robinson, C.J., et al. (2009). Introducing mothur: open-source, platform independent, community-supported software for describing and comparing microbial communities. Appl. Environ. Microbiol. *75*, 7537–7541. https://doi.org/10.1128/aem.01541-09.

Song, Z.-Q., Wang, L., Wang, F.-P., Jiang, H.-C., Chen, J.-Q., Zhou, E.-M., Liang, F., Xiao, X., and Li, W.-J. (2013). Abundance and diversity of archaeal accA gene in hot springs in Yunnan Province, China. Extremophiles *17*, 871–879. https://doi.org/10.1007/s00792-013-0570-4.

Spang, A., Poehlein, A., Offre, P., Zumbrägel, S., Haider, S., Rychlik, N., Nowka, B., Schmeisser, C., Lebedeva, E.V., Rattei, T., et al. (2012). The genome of the ammonia-oxidizing Candidatus Nitrososphaera gargensis: insights into metabolic versatility and environmental adaptations. Environ. Microbiol. *14*, 3122–3145. https://doi.org/10.1111/j.1462-2920.2012.02893.x.

Stewart, F.J., Ulloa, O., and DeLong, E.F. (2012). Microbial metatranscriptomics in a permanent marine oxygen minimum zone. Environ. Microbiol. *14*, 23–40. https://doi.org/10.1111/j.1462-2920.2010.02400.x.

Suess, E. (1980). Particulate organic carbon flux in the oceans—surface productivity and oxygen utilization. Nature *288*, 260–263. https://doi.org/10.1038/288260a0.

Tetu, S.G., Breakwell, K., Elbourne, L.D.H., Holmes, A.J., Gillings, M.R., and Paulsen, I.T. (2013). Life in the dark: metagenomic evidence that a microbial slime community is driven by inorganic nitrogen metabolism. ISME J. *7*, 1227–1236. https://doi.org/10.1038/ismej.2013.14.

Tolar, B.B., King, G.M., and Hollibaugh, J.T. (2013). An analysis of Thaumarchaeota populations from the northern gulf of Mexico. Front. Microbiol. *4*, 72. https://doi.org/10.3389/fmicb.2013.00072.

Tolar, B.B., Ross, M.J., Wallsgrove, N.J., Liu, Q., Aluwihare, L.I., Popp, B.N., and Hollibaugh, J.T. (2016). Contribution of ammonia oxidation to chemoautotrophy in Antarctic coastal waters. ISME J. *10*, 2605–2619. https://doi.org/10.1038/ismej.2016.61.

Tourna, M., Stieglmeier, M., Spang, A., Könneke, M., Schintlmeister, A., Urich, T., Engel, M., Schloter, M., Wagner, M., Richter, A., and Schleper, C. (2011). *Nitrososphaera viennensis* , an ammonia oxidizing archaeon from soil. Proc. Natl. Acad. Sci. U S A *108*, 8420–8425. https://doi.org/10.1073/pnas.1013488108.

Walker, C.B., de la Torre, J.R., Klotz, M.G., Urakawa, H., Pinel, N., Arp, D.J., Brochier-Armanet, C., Chain, P.S.G., Chan, P.P., Gollabgir, A., et al. (2010). *Nitrosopumilus maritimus* genome reveals unique mechanisms for nitrification and autotrophy in globally distributed marine crenarchaea. Proc. Natl. Acad. Sci. U S A *107*, 8818–8823. https://doi.org/10.1073/pnas.0913533107.

Ward, B.B. (2008). Chapter 5 - nitrification in marine systems. In Nitrogen in the Marine Environment, Second edition, D.G. Capone, D.A. Bronk, M.R. Mulholland, and E.J. Carpenter, eds. (Academic Press), pp. 199–261.

Wu, J., Guan, F., Wang, Y., Tan, Y., Yue, W., Wu, M., Bin, L., Wang, J., and Wen, J. (2016). A rapid and high-throughput microplate spectrophotometric method for field measurement of nitrate in seawater and freshwater. Sci. Rep. *6*, 20165. https://doi.org/10.1038/srep20165.

Xu, M.N., Li, X., Shi, D., Zhang, Y., Dai, M., Huang, T., Glibert, P.M., and Kao, S.-J. (2019). Coupled effect of substrate and light on assimilation and oxidation of regenerated nitrogen in the euphotic ocean. Limnol. Oceanogr. *64*, 1270–1283. https://doi.org/10.1002/lno.11114.

Yakimov, M.M., Cono, V.L., and Denaro, R. (2009). A first insight into the occurrence and expression of functional amoA and accA genes of autotrophic and ammonia-oxidizing bathypelagic Crenarchaeota of Tyrrhenian Sea. Deep Sea Res. Part Top. Stud. Oceanogr. *56*, 748–754. https://doi.org/10.1016/j.dsr2.2008.07.024.

Yakimov, M.M., Cono, V.L., Smedile, F., DeLuca, T.H., Juárez, S., Ciordia, S., Fernández, M., Albar, J.P., Ferrer, M., Golyshin, P.N., and Giuliano, L. (2011). Contribution of crenarchaeal autotrophic ammonia oxidizers to the dark primary production in Tyrrhenian deep waters (Central Mediterranean Sea). ISME J. *5*, 945–961. https://doi.org/10.1038/ismej.2010.197.

Yang, Y., Herbold, C.W., Jung, M.-Y., Qin, W., Cai, M., Du, H., Lin, J.-G., Li, X., Li, M., and Gu, J.-D. (2021). Survival strategies of ammonia-oxidizing archaea (AOA) in a full-scale WWTP treating mixed landfill leachate containing copper ions and operating at low-intensity of aeration. Water Res. *191*, 116798. https://doi.org/10.1016/j.watres.2020.116798.

Yool, A., Martin, A.P., Fernández, C., and Clark, D.R. (2007). The significance of nitrification for oceanic new production. Nature *447*, 999–1002. https://doi.org/10.1038/nature05885.

Zhang, C.L., Ye, Q., Huang, Z., Li, W., Chen, J., Song, Z., Zhao, W., Bagwell, C., Inskeep, W.P., Ross, C., et al. (2008). Global occurrence of archaeal *amoA* genes in terrestrial hot springs. Appl. Environ. Microbiol. *74*, 6417–6426. https://doi.org/10.1128/aem.00843-08.

Zhang, Y., Qin, W., Hou, L., Zakem, E.J., Wan, X., Zhao, Z., Liu, L., Hunt, K.A., Jiao, N., Kao, S.-J., et al. (2020). Nitrifier adaptation to low energy flux controls inventory of reduced nitrogen in the dark ocean. Proc. Natl. Acad. Sci. U S A *117*, 4823–4830. https://doi.org/10.1073/pnas.1912367117.

STAR★METHODS

KEY RESOURCES TABLE

REAGENT or RESOURCE	SOURCE	IDENTIFIER
Critical commercial assays		
Power Water DNA Isolation Kit	QIAGEN	Cat.14900-100-NF
GoTaq Green Master Mix	Promega	M7122
GoTaq qPCR Master Mix	Promega	A6001
VAHTS Universal Pro DNA Library Prep Kit	VAZYME	ND604
Deposited data		
The raw reads of ammonia monooxygenase subunit A (*amoA*) gene	This paper	Bioproject: PRJNA714789
The raw reads of acetyl-CoA carboxylase α-submit (*accA*) gene	This paper	Bioproject: PRJNA714983
Oligonucleotides		
Primer for AOA *amoA* gene, see Table S2	This paper	N/A
Primer for AOB *amoA* gene, see Table S2	This paper	N/A
Primer for AOA *accA* gene, see Table S2	This paper	N/A
Software and algorithms		
Mothur 1.40.5	Schloss et al. (2009)	https://mothur.org/
MEGA 7.0	Kumar et al. (2016)	https://www.megasoftware.net/
EvolView	He et al. (2016)	https://www.evolgenius.info/evolview/#/
OmicShare tools	http://www.omicshare.com/tools	http://www.omicshare.com/tools
SPSS Statistics 22.0	https://www.ibm.com/products/spss-statistics	https://www.ibm.com/products/spss-statistics
R 3.3.3	https://www.r-project.org/	https://www.r-project.org/
Canoco 5.0	http://www.canoco5.com/	http://www.canoco5.com/
Ocean data view 5.4.0	https://odv.awi.de	https://odv.awi.de
Matlab R2016a	https://www.mathworks.com/products/matlab.html	https://www.mathworks.com/products/matlab.html
Sigmaplot 12.5	https://systatsoftware.com/sigmaplot/	https://systatsoftware.com/sigmaplot/
Other		
Seabird conductivity–temperature–depth sensors	Sea-Bird Electronics	https://www.seabird.com/sbe-911plus-ctd/product?id=60761421595
0.22-μm pore-size polypropylene filters	Millipore	https://www.sigmaaldrich.com/US/en/substance/fluoroporemembranefilter1234598765
NanoDrop Lite	Thermo Fisher Scientific	https://www.thermofisher.com/order/catalog/product/ND-LITE-PR
Bio-Rad iQ5 Real-Time PCR system	Bio-Rad	https://www.bio-rad.com/
Veriti 96-Well PCR Thermal cycler	Applied Biosystems	https://www.thermofisher.com/order/catalog/product/4452300
Illumina sequencing	Illumina	Illumina MiSeq

RESOURCE AVAILABILITY

Lead contact

Further information and requests for resources should be directed to and will be fulfilled by the lead contact, Yiguo Hong (yghong@gzhu.edu.cn).

Material availability

This study did not generate new unique reagents.

Data and code availability

- The raw reads of *amoA* and *accA* gene sequences have been deposited in the NCBI short-read archive and are publicly available as of the date of publication. Accession numbers are listed in the key resources table.
- This paper does not report original code.
- Any additional information required to reanalyze the data reported in this paper is available from the lead contact upon request.

METHOD DETAILS

Sample collection and physicochemical parameters determination

Seawater samples were obtained in four water columns (S3, S7, S12 and S18) in the South China Sea (SCS) during the cruise in September 2016 on the R/V Shiyan 1. The sampling details are shown in Figure 1 and Table S1. Seawater samples were collected from Niskin bottles in Seabird conductivity–temperature–depth sensors (SBE-911 Plus CTD, Sea-Bird Electronics, USA) into HDPE plastic bottles. Water samples (2 L) were filtered by 0.22-μm pore-size polypropylene filters (47 mm diameter; Millipore, Billerica, MA, USA). And the membrane was immediately stored in liquid nitrogen. The temperature (°C) and salinity (‰) of the samples were continuously recorded by CTD. The dissolved oxygen (DO, μmol/L) was detected by the Winkler titration method (Chakraborty et al., 2016). The concentrations of dissolved inorganic nitrogen (DIN; NH_4^+, NO_2^- and NO_3^-) in seawaters were determined via the spectrophotometric detection methods described by Wu et al. (2016) and Guan et al. (2017).

DNA extraction and qPCR assay of *amoA* and *accA* genes

The total genomic DNA was extracted using the Power Water DNA Isolation Kit (Qiagen, Carlsbad, CA, USA) according to the manufacturer's instructions. The extracted total genomic DNA was dissolved in 50 μL of nuclease-free water. Qualities of the DNA were checked by spectrophotometric analysis using a NanoDrop Lite (Thermo Fisher Scientific, Wilmington, DE, USA) and electrophoresis was performed on a 1.0% agarose gel.

To quantify the abundances of AOA and AOB in the water columns of the SCS, qPCR assays were performed on a Bio-Rad iQ5 Real-Time PCR system (Bio-Rad, Hercules, CA, USA) by targeting AOA specific-*amoA* and AOB specific-*amoA* gene, respectively. The qPCR reactions were performed in triplicate with the following primers sets Arch-amoAF/Arch-amoAR for AOA (Francis et al., 2005) and amoA-1F/amoA-2R for AOB (Rotthauwe et al., 1997). In addition, the autotrophic potentials of AOA in water columns were estimated by quantifying the acetyl-CoA carboxylase α-submit (*accA*) gene, the specific and key carbon fixation gene of AOA. The qPCR reactions were performs in triplicate with primers set Crena_529F/Crena_981R (Yakimov et al., 2009). Further details concerning primers and qPCR conditions can be found in Table S2. In this study, the efficiency and correlation coefficients of q-PCR analysis ranged from 94.9%-101% and 0.989-0.995, respectively.

PCR amplification and high-throughput sequencing analysis

The *amoA* and *accA* genes of AOA were amplified by VeritiTM 96-Well PCR Thermal cycler (Applied Biosystems, Foster, CA, USA) using primer sets Arch-*amo*AF/ Arch-*amo*AR and Crena_529F/Crena_981R, respectively. The forward primers of Arch-*amo*AF and Crena_529F were attached to a unique 8 bp barcode sequence. The purification and pooling procedures of PCR products before submitting to the Genewiz facility were following the method described by Hong et al. (2021). VAHTS Universal Pro DNA Library Prep Kit for Illumina (Vazyme Biotech Co., Ltd.) was used to construct the clone library. Sequencing was performed using an Illumina MiSeq machine, which generating 250 bp paired-end reads. More details concerning the primers, PCR conditions and sequencing methods can be found in Table S2.

High-throughput sequencing was performed using Mothur software V1.40.5 (Schloss et al., 2009) according to the standard protocol. In brief, quality-controlled sequences were processed first by removing tags and primers. The *sub.sample* command was used to normalize data (all samples were analyzed at the same

sequencing depth). Sequences were simplified into those with the *unique.seqs* command and then aligned to newly developed two databases for *amoA* (He et al., 2018) and *accA* genes (unpublished data) with the *align.seqs* command. The *screen.seqs* command was used to screen and filter badly aligned sequences. To further reduce sequencing errors (i.e.; remove sequences which differ by one or more nucleotides) and remove chimeras, *pre.cluster*, *chimera.uchime*, and *remove.seqs* commands were employed. Taxonomic classification was conducted using the *classify.seqs* command with the newly developed databases and taxonomy file, and confidence cut-off was set to 85%. Sequences classified as "*unknown*" were removed using the *remove.lineage* command. Furthermore, sequences were clustered into operational taxonomic units (OTUs) using the *dist.seqs*, *cluster*, *make.shared*, and *classify.otu* commands. After comparing the similarities between *amoA*/*accA* gene sequences and 16S rRNA gene sequences of AOA, 11% (He et al., 2018) and 18% (unpublished data) dissimilarity level for *amoA* and *accA* genes were selected for clustering OTUs. A rarefaction curve was generated using the *rarefaction.single* command and rare OTUs (nseqs = 10) were removed via the *remove.rare* command. The *summary.single* command was used to obtain a table containing the number of sequences, sample coverage, observed OTUs, and diversity estimates. The sample coverage value refers to the coverage of each sample library and is used to evaluate the total number of community species represented by the sequencing results. Diversity indexes are the following: (1) Chao1 index, (2) Simpson index, (3) Shannon index, (4) Abundance-based coverage estimators (ACE) index, and (5) Evenness index. The Chao1 and ACE indexes are the two key estimators for calculating the community richness (the number of OTUs contained in a sample), which refers to the total number of species in a sample. The Shannon and Simpson diversity indexes take into account the number of species living in a habitat (richness) and their relative abundance (evenness). Evenness index provides information about the equity in species abundance in each sample. The coverage value refers to the coverage of each sample library and is used to evaluate the total number of community species represented by the sequencing results. Principal Coordinates (PCoA) plots were calculated using *pcoa* commands. Phylogenetic analysis of the representative *amoA* and *accA* gene sequences from each dominant OTU (top 7 and 14 OTUs for *amoA* and *accA* gene, covering 98.16% and 97.36% of the sequences) was conducted using MEGA7.0, EvolView software (He et al., 2016) and OmicShare tools (http://www.omicshare.com/tools). Heat maps were constructed in accordance with the abundance of dominant OTUs.

QUANTIFICATION AND STATISTICAL ANALYSIS

Statistical analysis

One-way analysis of variance (ANOVA) was performed using the software SPSS Statistics (version: 22.0) to compare the differences of the physicochemical properties and microbial characteristics. Pearson correlation was applied to examine the correlations between microbial characteristics and physicochemical parameters using the software R (version 3.3.3). Redundancy analysis (RDA) was performed using Canoco 5.0 software to analyze the archaeal communities and their correlations with physicochemical parameters. Principal coordinates analysis (PCoA) and heatmaps were used to visualize beta-diversity among samples. Ocean data view (ODV, https://odv.awi.de/en/software/download/), Matlab (version R2016a) and Sigmaplot (12.5) software were used for graphics.